

# A Novel Perception and Semantic Mapping Method for Robot Autonomy in Orchards

Yaoqiang Pan<sup>1</sup>, Hao Cao<sup>1</sup>, Kewei Hu<sup>1</sup>, Hanwen Kang<sup>1,\*</sup>, Xing Wang<sup>2,\*</sup>

<sup>1</sup> College of Engineering, South China Agriculture University, China

<sup>2</sup> Robotics and Autonomous System, IData61, CSIRO, Australia

\* Correspondence Authors

**Resumen**—In this work, we propose a novel framework for achieving robotic autonomy in orchards. It consists of two key steps: perception and semantic mapping. In the perception step, we introduce a 3D detection method that accurately identifies objects directly on point cloud maps. In the semantic mapping step, we develop a mapping module that constructs a visibility graph map by incorporating object-level information and terrain analysis. By combining these two steps, our framework improves the autonomy of agricultural robots in orchard environments. The accurate detection of objects and the construction of a semantic map enable the robot to navigate autonomously, perform tasks such as fruit harvesting, and acquire actionable information for efficient agricultural production.

## I. INTRODUCTION

Robot autonomy has become a key aspect of precision agriculture, which leverages the emerging robotics, sensor, and AI technologies to automate the process of scientific data collection [1], [2], yields estimation[3], [4], fruit growth monitoring[5], and fruits harvesting[6], [7]. Among the various subsystems of an intelligent agricultural robot, navigation is an essential component that enables the robot to operate autonomously in unstructured agriculture environments, like orchards and plantations [8]. It comprises two essential steps: mapping and motion planning. The first step aims to model orchards enabling robots to comprehensively understand the environment where they are operating. The second step plans the motions on the map for the robot to accomplish its tasks. In summary, an accurate and effective representation of environments is key to achieving robot autonomy.

Simultaneous location and mapping (SLAM) technology is a basic technique that has been widely utilised in self-positioning and map construction for robotic autonomy in the field. It applies sensors such as cameras, Light Detection and Range (Lidar), radar, and IMU to acquire visual and kinetic information from their surroundings. At the front end of the SLAM, the information will be used to compute the odometry of their motion and can be used to construct the map of the surrounding environments. At the back end of the SLAM, the map of the environments will be fine-tuned by close-loop detection and overall map optimisation. Then, an accurate landmark or point cloud map can be obtained. Traditional SLAM focuses on extracting robust low-level geometry features to establish the right correspondence and compute the correct transient pose while lacking the ability to extract

information and understand the environments that they are currently building. Therefore, traditional SLAM can only provide raw geometries that do not include any semantic information, which limits its utilisation in autonomous operations. Having additional semantic information can significantly increase the capability of the robotics application. For example, in an orchard, if the robot knows where the target fruit trees are, it can automatically find its path to the given position and finish the work, rather than having a human click on the screen each time to tell the robot specifically where to go.

The increasing demand for higher levels of autonomy in agricultural production places high demands on the robot's ability to understand its environment [9]. To achieve this goal, robots need to recognise information about objects in the scene and find out their locations on the map. That is, based on the original map from the SLAM, a semantic map is created that represents the environment using a set of semantically meaningful objects. This representation facilitates large-scale autonomy and the acquisition of actionable information in highly unstructured orchard environments because it is memory efficient, less ambiguous, and more informative. Deep learning, is an emerging and powerful tool for processing and extracting semantic information from input sensors' reading [10].

Although significant progress has been made in the construction of semantic maps using 2D image data or pseudo-3D point cloud data, semantic mapping methods directly on 3D point cloud data have not yet been widely explored. Compared with the semantic processing on 2D image data or pseudo-3D point cloud data, the semantic processing on 3D point cloud data can directly use the output of SLAM and does not require any additional calibration or data format conversion, which avoids numerical errors and large computational consumption. However, due to the unstructured and sparse nature of 3D point clouds, efficiently processing semantic information within point clouds remains challenging.

In this work, by taking advantage of LiDAR-based mapping methods, a novel framework including two-step perception and semantic mapping is proposed to achieve robotic autonomy in orchards. First, we present a novel 3D detection method to accurately identify and localise objects on point cloud maps directly. Second, we develop a mapping module to construct a visibility graph map of orchards based on the extracted

object-level information and terrain analysis. Specifically, our contributions are as follows.

- Create a fast and accurate 3D Object Detection Network (3D-ODN) to process 3D point cloud from SLAM.
- Develop a novel semantic mapping framework for orchard modelling by using information from the 3D-ODN and terrain analysis.
- Demonstrate the proposed perception and semantic mapping framework on mobile robots in orchards.

The rest of this paper is organised as follows. Section II surveys related work, followed by the proposed methodologies in Section III. Section III-A overviews the system setup of our approach, Section III-B introduces the architecture and implementation of the 3D-TDN, while Section III-C introduces the method of the semantic mapping framework. The experimental results and discussions are given in Sections IV. and then the conclusions are given in Section V.

## II. RELATED WORKS

### II-A. Review on 3D detection

Although great success has been achieved in the target detection of two-dimensional images in recent years, target detection based on three-dimensional point clouds is still an open and challenging field [11]. Compared with three-dimensional point clouds, two-dimensional images cannot describe the spatial distribution of objects in detail, especially in scenes where there are occlusions and overlapping objects with the complex spatial distribution. Target detection based on three-dimensional point clouds has begun to receive more and more attention. Tao et al. put forward a kind based on improved F-PointNet and three-dimensional clustering method to detect positioning method of mature pomegranate fruit[12]. The method includes: (1) using RGB - D feature fusion Mask R-CNN implementation fruit detection and segmentation; (2) combining PointNetOPTICS algorithm, point cloud segmentation of fruit area and placing a three-dimensional box; and (3) sphere fitting to achieve the size and location of the pomegranate.

Chen et al. proposed performed a deep learning framework directly processing the forest point clouds to realize the ITC segmentation[13]. This method first subdivides the point cloud into multiple voxels and then uses PointNet to identify the tree crown at the voxel scale. Finally, the highly correlated gradient information is used to obtain the boundaries of each canopy. Wei et al. proposed a new point cloud segmentation network, BushNet.[14]. The minimum probability random sampling module is used to quickly sample huge point clouds, and the local multi-dimensional feature fusion module makes the network more sensitive to shrub point cloud features. The multi-channel attention module achieves network attention distribution and improves training efficiency. This work proposes a 3D-ODN model that includes three steps: space subdivision, feature encoder, and detection network. The 3D-ODN model takes point clouds as inputs and estimates the bounding box of the elements in the orchards (fruit trees in our work).

The basic idea is to extract geometry features in BEV angle and transfer the 3D point cloud map into a 2D pseudo- image. Then, the 2D pseudo-images will be fed into the detection network to detect the objects in a much faster and more efficient way.

### II-B. Review on Semantic SLAM

Semantic SLAM enhances the capabilities of the SLAM system by integrating semantic information. It not only focuses on the geometric structure of the environment but also incorporates the semantic information of objects into the mapping and localization process. This semantic information can include knowledge about object categories, properties, shapes, motion states, and more. By performing semantic segmentation and recognition of objects in the mapping process, Semantic SLAM can provide robots with richer and more meaningful maps, enabling them to better understand and interact with the environment. Bowman et al. proposed a probabilistic data association-based method for semantic SLAM, which tightly couples inertial, geometric, and semantic observations into a single optimization framework. The joint measurement SLAM problem is decomposed into the continuous pose and discrete data association and semantic label optimization sub-problems. [15]. Ouyang et al. proposed the semantic SLAM method, which introduces interactive SLAM to optimize the pose of point clouds. Through a point cloud segmentation model, the semantic information of point clouds is obtained and the positioning accuracy is optimized.[16]. BAVLE et al. proposed a lightweight real-time visual semantic SLAM framework. This method combines low-level visual/visual-inertial odometry (VO/VIO) with planar geometric information extracted from detected semantic objects to generate a sparse environmental semantic map while estimating the complete 6-degree of freedom pose of the robot.[17]. Although the above individuals utilized semantic information to assist in localization and mapping during the SLAM process, they did not ultimately construct a dense map containing semantic information suitable for autonomous driving navigation.

Li et al. proposed a new semantic-assisted lidar SLAM with closed-loop based on LOAM, SA-LOAM, which utilizes semantics from odometers and closed-loop detection for semantic matching, downsampling, and planar constraints, and can construct globally consistent semantic maps in large-scale scenes.[18]. Wan et al. proposed a lightweight indoor semantic map construction algorithm named NGLSFusion that does not use GPUs. In the semantic graph construction method, the pre-trained model of the lightweight network LinkNet was optimized to provide semantic information. Use OctoMap and Voxelblox to fuse semantic point clouds. Obtain a structurally complete reconstructed semantic graph.[19]. The semantics in the map constructed by the above individuals are not specific to a specific object, and their semantics are only a set of points with category information. This work applies the semantic SLAM to enhance the capabilities of the traditional SLAM system. Additionally, the specific object information is utilised in the semantic SLAM from the 3D objective detection

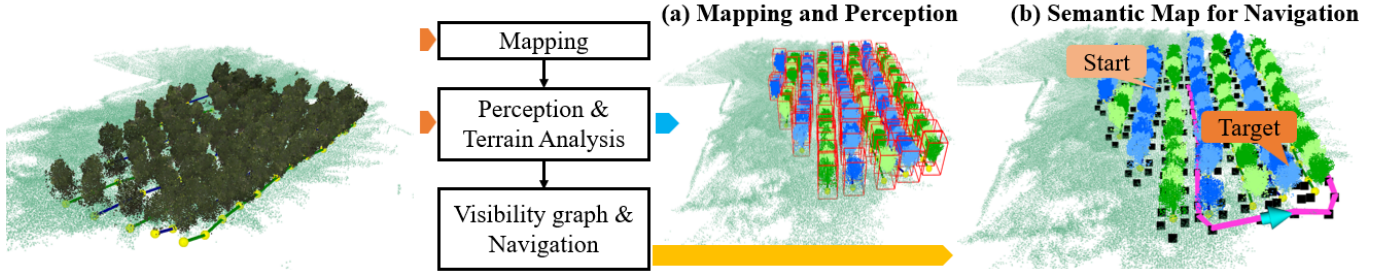


Figure 1. System-overview (a) Mapping and Perception (b) Semantic Map for Navigation

network rather than having pure category information. Finally, our work generates a dense map from the semantic SLAM and demonstrates its suitability during autonomous driving navigation.

### III. METHODS

#### III-A. System overview



Figure 2. Mobile Robot (a) AGX-HUNTER (b) ST-100

The framework of the proposed perception and semantic mapping framework is shown in Figure 1. The framework can be divided into three steps, which are mapping, perception, and semantic processing on a map. Firstly, the orchard data is collected by a mobile robot with Lidar in either tel-control or an autonomous way. The mapping procedure is accomplished by using LiDAR odometry and mapping algorithms on the acquired data. After that, the fruit trees of the orchards can be detected and localised by the 3D-ODN model using the geometry information within the map. Next, a semantic processing module that can extract terrain and topological information is developed and utilised here to construct the semantic map. Finally, the constructed semantic map includes information on each fruit tree that can be used to plan autonomous operations and a node connection map that can navigate robots to access each fruit tree within the map.

**Hardware and Software:** The overall hardware and software configuration on our developed mobile robot to perform semantic mapping of orchards are shown in Figure 2 and Figure 3, respectively. The sensor kit on the mobile robot (AGX Hunter-SE or ST-100 base) includes a 32-line RoboSense Lidar (RS-Helios), a Livox-Avia Lidar, a Realsense-

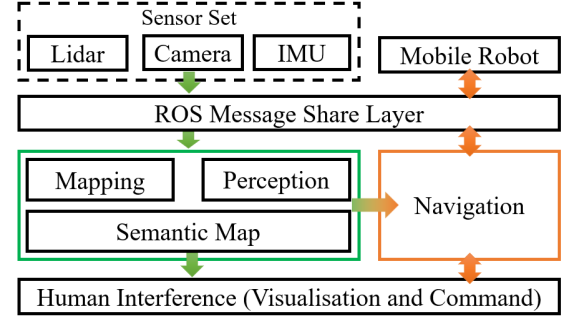


Figure 3. software architecture of system

D435 depth camera, and an external IMU (9-axis). The data acquisition frequency of the RS-Helios, Livox-Avia, and IMU are 20Hz, 10 HZ, and 400HZ, respectively. We only acquire colour images from the Realsense D435 camera and the data acquisition frequency is 30 HZ. The data acquired by the sensors can be used to build the initial point cloud maps of orchards by using a mapping algorithm. For our case, we use Lio-SAM to build the point cloud map of orchards with the data from the RS-Helios. While for the Livox-Avia Lidar, the R3-LIVE algorithm is used to build the map. The sensor kit on the robot is connected to the central computer (Nvidia Xavier) using the Robot Operating System (ROS Noetic) in Ubuntu 20.04. The data transmission from the RS-Helios and Livox Avia to the central computer is through an Ethernet port, by using rslidar-ros-driver and Livox-ros-driver, respectively. The neural network model is programmed based on PyTorch 1.7. Its training is performed on NVIDIA RTX-3090, while forward inference is tested on both NVIDIA RTX-3090 and NVIDIA Xavier.

#### III-B. Perception Model

**3D-ODN:** A novel perception model on a 3D point cloud map based on a one-stage detection network is proposed. As shown in Figure 4, the 3D-ODN model includes three steps: space subdivision, feature encoder, and detection network. The 3D-ODN model takes point clouds as inputs and estimates the bounding box of the elements in the orchards (fruit trees in our work). Firstly, the map will be subdivided into numbers of evenly-spaced and certain-sized local maps. Each subdivided local map then will be fed into a feature encoder. The basic

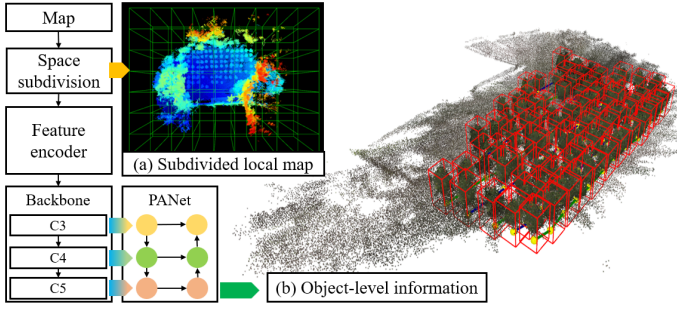


Figure 4. network architecture of tree detection

idea of this step aims to extract geometry features in BEV angle and transfer the 3D point cloud map into a 2D pseudo-image. Then, the 2D pseudo-images will be fed into the detection network to detect the objects. The output will be generated by combining the results from all subdivided grids.

**Space Subdivision:** To efficiently extract and process the geometric details in 3D geometry, a space subdivision strategy is utilised to divide a certain-sized local map from the global map (we choose 10m in this work). However, such an approach encounters an implementation issue during experiments. That is, some fruit trees only have parts of their shape on the local map due to space subdivision. To solve this, we proposed a sliding window detection method. After detecting a 10m x 10m local point cloud map, we move the window in the positive X-axis direction by 8m in each step. This is because, based on our measurement, the maximum forward sliding distance in the radius of the fruit trees is less than 2m, so the distance of each sliding window should be 8m (10m minus the diameter of the tree crown). This sliding window approach ensures the fruit trees that are not fully covered by the last local sliding map will be fully included in the next window. The sliding window will be repeatedly moved to X-axis and Y-axis until all the areas of the global map have been traversed. Some fruit trees may have multiple predictions due to being covered by multiple subdivided local maps. The Non-Maximum Suppression (NMS) is used here to find the predictions with the highest confidence and remove overlapping predictions.

**Feature Encoding:** To leverage a 2D detection network to process point cloud information, we first convert a point cloud to a 2D pseudo image. That is, the local point cloud will be transferred to the BEV angle and divided into evenly-spaced grids on the x-y plane. This step creates a list of pillars with the ultimate extent on the z-axis direction. The points within each pillar will be used to extract features of the local geometry. In this work, we utilise Viewpoint Feature Histogram (VFH) [20] and PointNet [21] to perform feature extraction. The size of each pillar is 0.5m and 0.5m in the x and y directions, respectively. Some pillars are empty or only have a very small number of points due to the sparsity of the point cloud. Therefore, we apply a requirement that only the pillars with a point number large than 100 will be used to

extract features. In this way, a 3D point cloud is converted into a 2D pseudo image.

**Network Architecture:** we leverage a one-stage detection network architecture to perform object-level information perception on local maps. The network utilises ResNet-50 as the backbone. The input of the backbone is the encoded features of the subdivided local map from the feature encoder. Then, the feature maps from the C3, C4, and C5 levels of the backbone are used to construct the multi-scale feature pyramid network. In this work, the Path Aggregation Network (PANet) [22] is used here to enhance the multi-scale image feature extraction and processing. Then, the processed feature maps from the PANet are used to perform detection. The combined detection results from the C3, C4, and C5 level of the PANet forms the predicted objects. NMS is then used at the final to filter the prediction and generate the final results for map perception.

### III-C. Semantic Mapping

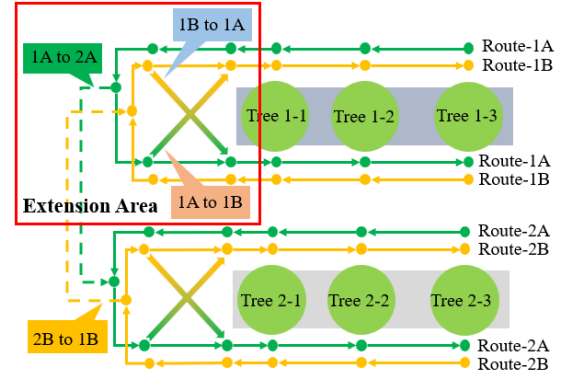


Figure 5. Semantic mapping

**Mapping:** The mapping process is performed by using either the Lio-sam [23] or R3live [24]. For mapping using Lio-sam, the RS-Helios and external IMU (400 hz) are used. We do not use GPS in Lio-sam Mapping since the obstacles in orchards will affect the stability and accuracy of the GPS signal. For mapping by using the R3live, the Livox-avia, internal IMU of livox-avia, and RGB camera are used. Both Lio-sam and R3live can perform well in modelling and describing the geometry properties of the orchards. Comparably, since R3live can provide a map colourisation function for visualisation. The colour map of the orchard is shown in Figure 6 (a). We can see that the global map of the orchard is highly unstructured. In the meantime, points within the map are highly unevenly distributed.

**Perception and terrain Analysis:** The acquired map is then processed by the perception and terrain analysis. That is, we first utilise the 3D-ODN model to perform detection on the global map. This step will generate the list of detected fruit trees. Then, a terrain analysis method based on the Cloth Simulation Filtering (CSF) algorithm [25] is utilised here to find the ground and obstacles of the orchards. The parameter of the CSF can be adjusted accordingly based on different terrain (we set  $dT=0.15$  and the iteration number as 100,



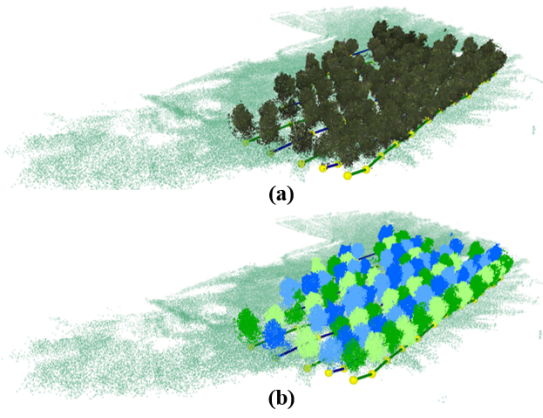


Figure 6. Map colourisation for visualisation

respectively). In this way, the points of the global map are separated into traversable terrains and obstacles. By further combining the perception results of fruit trees, the points of the global map are classified into three classes: fruit trees, traversable terrains, and other obstacles. The perception and terrain analysis can be either operated online in an onboard computer on a real-time data stream or offline using the recorded data.

**Visibility graph:** The generated perception and terrain analysis results cannot be directly utilised to navigate the robot in the orchard. This step aims to build the navigation map for robot autonomy by giving the semantic information about the orchard. Firstly, by giving the position of each tree on the map, the Hough line detection algorithm is used to find the column of the tree. The terrain between the adjacent tree columns is the corridor that the robot can transverse. Then, for each tree, we define two access points (with different forward directions) for each tree at each side of the tree column, as shown in Figure 5. The node with the same direction will be connected as the loop around the tree column. For each of the three columns, there are two routes with different moving directions. To allow the robot to change its moving direction (switch the route), the robot can switch its route at the extension area of the column. Meanwhile, the robot can also plan its motion from one tree column to another tree column through the connection between the route of different columns. In this way, by using the information from the semantic information, we convert the unstructured orchard environments into a structured graph map with nodes (via points) and edges (the connection between via points). This step will be conducted after the finish of the mapping procedure. Given the results of the perception and terrain analysis, the graph map of orchard navigation will be automatically constructed accordingly.

## IV. EXPERIMENT AND DISCUSSION

### IV-A. Data collection and Experimental methods

During the experiments, we first manually control the robot to go through the orchards and create a closed-loop path. The lidar data, camera data, and IMU data were collected

to generate the global point cloud map of the orchard. Data collection was conducted in the public experimental orchard at South China Agricultural University from 10:00 am to 4:00 pm, during which the distance between the tree trunks ranged from 1.2 to 2.5m, and the maximum distance from the ground to the top of the canopy was between 3.3 and 4.5m. Three orchards were included and surveyed for dataset creation. The open-source software pcd-annotation, available on GitHub, was used to annotate the trees in the maps by creating bounding boxes on each of the trees.

We conducted three experiments to evaluate the proposed method. The first experiment analysed the effect of local maps of different sizes on the detection performance of the network. The second experiment compared the efficiency and accuracy of different feature extraction methods. The third experiment involved the real-time detection of fruit trees in an entire orchard using a mobile platform. Each network was trained three times and the best-performing network weight, based on verification accuracy, was saved for evaluation. We evaluated the detection performance using mIoU (mean intersection over union), map (mean average precision) and detection time on the same orchard map. The dataset for training the network was created using 90 % of the local maps from five orchard scenes, while the remaining 10 % was used for training verification and evaluation. To enhance the data, the x, y and z directions of each local point cloud map were randomly scaled between 0 and 1, resulting in a total of 3000 enhanced local maps.

### IV-B. Ablation study of Perception

Table 1

strategy	Voxel Specification Strategy		
	feature map time (s)	Predict time (s)	miou
5m*5m+64*64	0.0398	0.0168	0.809
10m*10m+64*64	0.1583	0.0168	0.798
20m*20m+64*64	0.6275	0.0168	0.772
5m*5m+128*128	0.0425	0.0268	0.725
10m*10m+128*128	0.1681	0.0268	0.812
20m*20m+128*128	0.6315	0.0268	0.796

**Evaluation on Subdivision:** Table IV-B shows the evaluation of the efficiency of network operation using different scales and resolutions of local maps on the YOLO-3D model. The resolutions tested were 64, 128 and 256 for planarization. Experiments 1, 2 and 3 compared the impact on network performance of 5m x 5m, 10m x 10m and 15m x 15m local maps when converted to 128 x 128 feature maps using density, mean height and normal vector. The experimental results show that the size of the local map has a significant impact on the processing time of the point cloud planarization. Larger maps require more time due to the increased number of point cloud points to be processed. The 5m x 5m map has the shortest processing time with an average of 0.0168s, while the 15m x 15m map has the longest processing time with an average of 0.0268s. However, the 10m x 10m map achieves the highest IoU. For the same planarization resolution, smaller maps represent a smaller area per voxel. This results in more

pixels corresponding to the point cloud representing fruit trees, making the fruit tree features more prominent and improving detection accuracy. Therefore, the IoU of the 10m x 10m map is higher than that of the 15m x 15m map. However, the IoU of the 5m x 5m map decreases. When the point cloud of fruit trees in the 5m x 5m map is converted to a feature map, holes appear in the representation. These holes negatively affect the IoU of the network prediction frame.

Tests 2, 4 and 5 investigated the effect of different resolutions on network performance. The results show that resolution size has a minimal impact on the feature extraction stage, but a significant impact on the time spent in the network prediction stage. Higher resolutions result in larger feature maps entering the network, requiring more parameters for prediction, which directly affects the prediction stage. High resolutions can introduce holes in the fruit tree pixels of the feature map, affecting the accuracy of the prediction. Conversely, too low a resolution will result in reduced feature information and reduced recognition accuracy. Considering both accuracy and time, it is advisable to select a local map size of 10m x 10m and a feature map resolution of 128 x 128 as the input to the network. This configuration strikes a balance between accuracy and computational efficiency.

**Table 2**

Feature extraction strategy			
strategy	feature map time (s)	Prediction time (s)	miou
vfh	2.13	0.0592	0.824
Proposed method	0.1681	0.0268	0.812
pointnet++	\	0.517	0.798
pointnet++	\	0.943	0.824
pointnet++	\	1.39	0.843

**Evaluation on Encoder:** In this section, different feature extraction strategies were evaluated during network training to assess the recognition accuracy of the model. The View Feature Histogram (VFH) descriptor, derived from the Fast Point Feature Histogram (FPFH), was used as one of the feature extraction methods. VFH allows global feature extraction from the input point cloud, producing a 308-dimensional descriptor that captures view direction and surface shape components from the extended FPFH. **Test 1** used VFH for feature extraction. The local map was voxelized along the x and y directions and VFH calculations were performed on the groups of points within each voxel. The resulting 308 descriptor parameters were stored in a 128x128 feature map with 308 channels. This process was repeated for all voxels, resulting in a 308x128x128 feature map for each local map. The yolov7 network was modified to accept 308 channels as input and predictions were made accordingly. **Test 2** used a feature extraction method proposed in the paper. The average height, density and angle between the normal vector and the z-axis of the groups of points within each voxel were used as features and assigned to three channels. After extracting features from the local map, a 3x128x128 feature map was generated and fed into the yolov7 network for prediction. For comparison, **Test 3** used PointNet++ to

detect fruit tree point clouds. PointNet++ used individual point labelling annotations, requiring a separate manually labelled dataset for training. The Intersection over Union (IoU) was calculated by comparing the bounding box of the predicted fruit tree point cloud with the annotated box from the dataset used to train the yolov7 network. This evaluation allowed a comparison of the detection performance achieved using different feature extraction methods and networks.

Tests 1 and 2 demonstrated that the use of VFH descriptors as point cloud features in voxels allows a better representation of the fruit tree point cloud structure distribution, resulting in improved detection performance by the YOLO-3D network. The IOU obtained using VFH descriptors was higher (0.824) than the method proposed in the paper. However, the method proposed in the paper outperformed VFH in terms of network efficiency at both the feature extraction and prediction stages. The VFH descriptors require more computation due to their 308 parameters compared to the average height, density and normal vector angle used in the proposed method. In addition, the 308-channel feature map of VFH also requires more computations than the three-channel feature map proposed in the paper.

In tests 3, 4 and 5, PointNet++ was used for fruit tree point cloud detection with 1000, 2500 and 5000 sampling points respectively, along with the MSG feature extraction method. PointNet++ achieved the highest accuracy of all tests. However, considering that the local map is a point cloud in a 10m x 10m space, even after removing ground points with the CSF algorithm, the average number of points per local map remains around 10,000. While setting a lower number of sampling points can improve the operational efficiency of PointNet++, the fruit tree feature might not be extracted well, leading to reduced prediction accuracy. Setting the number of sampling points to 2500 and 5000 significantly improved the detection accuracy of PointNet++, but with a cost of longer run times, which may be unacceptable.

#### IV-C. Perception in Orchards

We further evaluate the 3D-ODN in real-time detection together with the Lio-sam algorithm. During the mapping process, the Lidar point cloud matched each time will be the registered topic and released, and the real-time position and posture of the robot in the coordinate system with the starting point as the origin will also be updated in real-time. This experiment is conducted through subscription/cloud. The registered topic obtains the orchard point cloud output by Lio-sam for each frame. By setting the range of the orchard, the non-orchard points outside the range are removed, and the point cloud of each frame is classified into each 5 m \* 5 m local map. According to the position and posture output by Lio-sam, the 10 m \* 10 m local map is extracted for fruit tree point cloud detection.

The robot moves at an average speed of 1 m/s under human control. When the robot is about to reach the edge of the first line of a 5 m \* 5 m local map of a 10 m \* 10 m local map, the two local 5 m \* 5 m local maps that have been detected and are

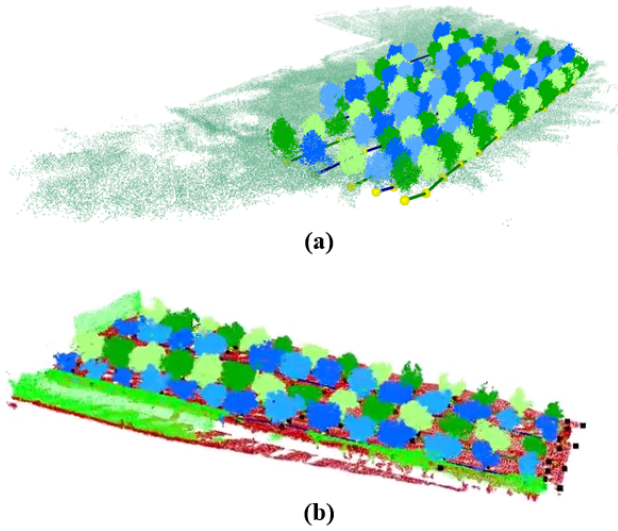


Figura 7. Semantic Results in Orchards

about to enter and the two local  $5\text{ m} \times 5\text{ m}$  local maps that are not detected in the forward direction will form a  $10\text{ m} \times 10\text{ m}$  local map for detection. With the robot as the centre, the local map divided by  $5\text{ m} \times 5\text{ m}$  in the positive and negative directions of the  $x$  and  $y$  axes is known about the distribution of fruit trees. In the process of fruit tree detection, while the robot is building a map, the average time for fruit tree detection on a  $10\text{ m} \times 10\text{ m}$  local map is  $0.65\text{ s}$ , while the maximum distance for the robot to walk at full speed is  $0.65\text{ m}$ , so the fruit tree detection within  $5\text{ m}$  meets the obstacle avoidance requirements of the robot.

#### IV-D. Navigation on Semantic Map

With the constructed visibility graph of the orchards, we can plan the robot's motion in the orchards. Firstly, we use a Lidar-based relocalisation algorithm to find the real-time pose of the robot on the map. Dijkstra is then used to find the global path from the current robot to the goal. A local motion planner is used to receive the global path and compute the velocity command to control the robots. Several examples of results are shown in Figure. From the experiments, our methods show superior robustness to find the feasible path for robot navigation in the orchards, as shown in Figure 8.

#### IV-E. Discussion

This paper presents a two-stage perceptual and semantic mapping framework based on deep learning for orchard environments. The framework involves dividing the LiDAR-derived orchard map into local maps and performing feature extraction on each local map. A deep learning network is then used to detect orchard targets, and the detection results are mapped onto the global map. The framework extracts various semantic information from the global point cloud map,

including individual fruit tree point clouds, tree line information, spatial location information of fruit trees, orchard terrain, obstacles, and accessible areas for autonomous vehicles.

The experiments compared different feature extraction methods. The results showed that the VFH feature extraction method is more favourable for network prediction, although it has an operation time of  $2.13$  seconds, which can be considered unacceptable. On the other hand, the method proposed in this paper, which uses density, average height and principal angle to form a feature map, has a shorter processing time of only  $0.1949$  seconds, while still achieving a good balance between speed and performance. Experiments were also carried out to determine the most appropriate settings for local map size and feature map resolution. The results showed that a local map size of  $10\text{ m} \times 10\text{ m}$  and a feature map resolution of  $128 \times 128$  achieved the highest detection accuracy, with a mean intersection over union (mIoU) of  $0.812$ . Based on these results, the proposed method enables direct detection of fruit trees from 3D point clouds, offering a combination of performance and accuracy. It provides real-time perception capabilities for autonomous vehicles in orchard environments and facilitates the automated construction of semantic maps for orchards.

## V. CONCLUSION

This work presents a new method for perception and semantic mapping in orchards using deep learning techniques. We use a lidar-based mapping method to reconstruct a point cloud map, from the natural orchard. Then, a novel perception method on a 3D point cloud map is developed to perform 3D object detection on the reconstructed map. Furthermore, a visibility graph is constructed based on the geometrical and semantic information of the map. The experiments show that our proposed perception and semantic mapping frameworks can efficiently detect trees at different scales and different voxel resolutions. A  $10\text{ m} \times 10\text{ m}$  local map with  $128 \times 128$  resolution can achieve a balance between network performance and efficiency. Moreover, the final constructed visibility graph can provide strong global planning capability to enable robot autonomy in unstructured orchard environments. The future research direction outlined by the authors includes the cooperative operation of aerial robots, better terrain analysis, and local motion planning.

## ACKNOWLEDGMENTS

The author thanks the financial support of the Guangzhou Science and Technology Plan project (2023B01J0046).

## REFERENCIAS

- [1] H. Kang and C. Chen, "Fast implementation of real-time fruit detection in apple orchards using deep learning," *Computers and Electronics in Agriculture*, vol. 168, p. 105108, 2020.
- [2] L. Fu, F. Gao, J. Wu, R. Li, M. Karkee, and Q. Zhang, "Application of consumer rgb-d cameras for fruit detection and localization in field: A critical review," *Computers and Electronics in Agriculture*, vol. 177, p. 105687, 2020.
- [3] T. Liu, H. Kang, and C. Chen, "Orb-livox: A real-time dynamic system for fruit detection and localization," *Computers and Electronics in Agriculture*, vol. 209, p. 107834, 2023.



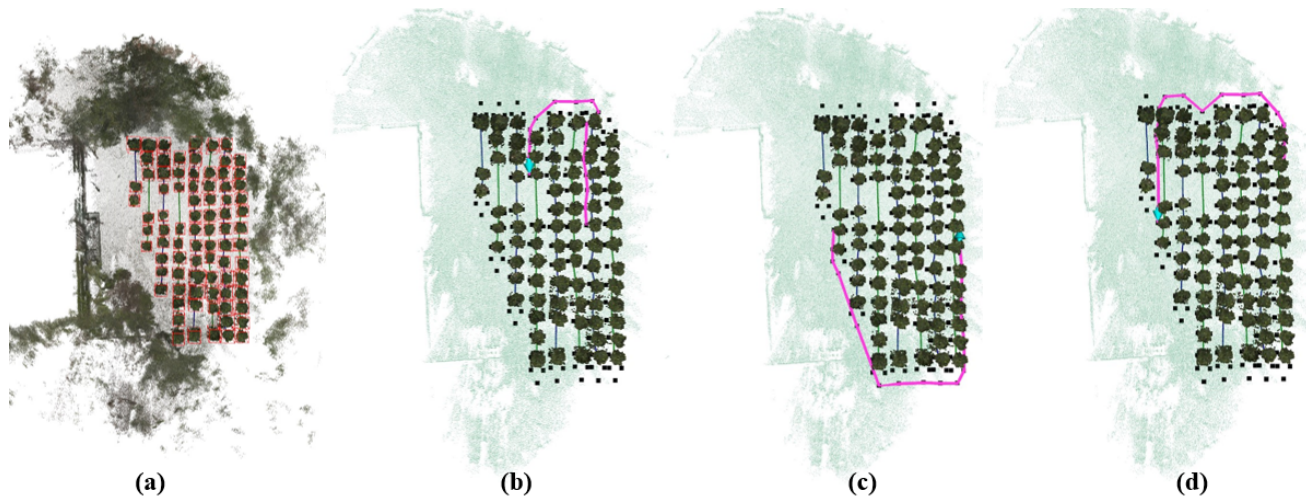


Figura 8. (a) Global Orchard Detection Results (b) Example 1 of local motion planning (c) Example 2 of local motion planning (d) Example 3 of local motion planning

- [4] Z. Zhou, Z. Song, L. Fu, F. Gao, R. Li, and Y. Cui, "Real-time kiwifruit detection in orchard using deep learning on android™ smartphones for yield estimation," *Computers and Electronics in Agriculture*, vol. 179, p. 105856, 2020.
- [5] L. F. Oliveira, A. P. Moreira, and M. F. Silva, "Advances in agriculture robotics: A state-of-the-art review and challenges ahead," *Robotics*, vol. 10, no. 2, p. 52, 2021.
- [6] X. Wang, H. Kang, H. Zhou, W. Au, M. Y. Wang, and C. Chen, "Development and evaluation of a robust soft robotic gripper for apple harvesting," *Computers and Electronics in Agriculture*, vol. 204, p. 107552, 2023.
- [7] H. Kang, X. Wang, and C. Chen, "Accurate fruit localisation using high resolution lidar-camera fusion and instance segmentation," *Computers and Electronics in Agriculture*, vol. 203, p. 107450, 2022.
- [8] H. Zhou, X. Wang, W. Au, H. Kang, and C. Chen, "Intelligent robots for fruit harvesting: Recent developments and future challenges," *Precision Agriculture*, vol. 23, no. 5, pp. 1856–1907, 2022.
- [9] H. Kang and X. Wang, "Semantic segmentation of fruits on multi-sensor fused data in natural orchards," *Computers and Electronics in Agriculture*, vol. 204, p. 107569, 2023.
- [10] X. Wang, H. Kang, H. Zhou, W. Au, and C. Chen, "Geometry-aware fruit grasping estimation for robotic harvesting in apple orchards," *Computers and Electronics in Agriculture*, vol. 193, p. 106716, 2022.
- [11] G. Lin, Y. Tang, X. Zou, J. Xiong, and Y. Fang, "Color-, depth-, and shape-based 3d fruit detection," *Precision Agriculture*, vol. 21, pp. 1–17, 2020.
- [12] T. Yu, C. Hu, Y. Xie, J. Liu, and P. Li, "Mature pomegranate fruit detection and location combining improved f-pointnet with 3d point cloud clustering in orchard," *Computers and Electronics in Agriculture*, vol. 200, p. 107233, 2022.
- [13] X. Chen, K. Jiang, Y. Zhu, X. Wang, and T. Yun, "Individual tree crown segmentation directly from uav-borne lidar data using the pointnet of deep learning," *Forests*, no. 2, 2021.
- [14] H. Wei, E. Xu, J. Zhang, Y. Meng, J. Wei, Z. Dong, and Z. Li, "Bushnet: Effective semantic segmentation of bush in large-scale point clouds," *Computers and Electronics in Agriculture*, vol. 193, p. 106653, 2022.
- [15] S. L. Bowman, N. Atanasov, K. Daniilidis, and G. J. Pappas, "Probabilistic data association for semantic slam," in *2017 IEEE international conference on robotics and automation (ICRA)*. IEEE, 2017, pp. 1722–1729.
- [16] Z. Ouyang, C. Zhang, and J. Cui, "Semantic slam for mobile robot with human-in-the-loop," in *Collaborative Computing: Networking, Applications and Worksharing: 18th EAI International Conference, CollaborateCom 2022, Hangzhou, China, October 15-16, 2022, Proceedings, Part II*. Springer, 2023, pp. 289–305.
- [17] H. Bavle, P. Puente, J. How, and P. Campoy, "Vps-slam: Visual planar semantic slam for aerial robotic systems," *IEEE Access*, vol. PP, no. 99, pp. 1–1, 2020.
- [18] L. Li, X. Kong, X. Zhao, W. Li, F. Wen, H. Zhang, and Y. Liu, "Sa-loam: Semantic-aided lidar slam with loop closure," 2021.
- [19] L. Wan, L. Jiang, B. Tang, Y. Li, B. Lei, and H. Liu, "Nglfusion: Non-use gpu lightweight indoor semantic slam," *Applied Sciences*, vol. 13, no. 9, p. 5285, 2023.
- [20] R. B. Rusu, G. Bradski, R. Thibaux, and J. Hsu, "Fast 3d recognition and pose using the viewpoint feature histogram," in *2010 IEEE/RSJ International Conference on Intelligent Robots and Systems*. IEEE, 2010, pp. 2155–2162.
- [21] C. R. Qi, H. Su, K. Mo, and L. J. Guibas, "Pointnet: Deep learning on point sets for 3d classification and segmentation," in *Proceedings of the IEEE conference on computer vision and pattern recognition*, 2017, pp. 652–660.
- [22] S. Liu, L. Qi, H. Qin, J. Shi, and J. Jia, "Path aggregation network for instance segmentation," in *Proceedings of the IEEE conference on computer vision and pattern recognition*, 2018, pp. 8759–8768.
- [23] T. Shan, B. Englot, D. Meyers, W. Wang, C. Ratti, and D. Rus, "Lio-sam: Tightly-coupled lidar inertial odometry via smoothing and mapping," in *2020 IEEE/RSJ international conference on intelligent robots and systems (IROS)*. IEEE, 2020, pp. 5135–5142.
- [24] J. Lin and F. Zhang, "R 3 live: A robust, real-time, rgb-colored, lidar-inertial-visual tightly-coupled state estimation and mapping package," in *2022 International Conference on Robotics and Automation (ICRA)*. IEEE, 2022, pp. 10 672–10 678.
- [25] W. Zhang, J. Qi, P. Wan, H. Wang, D. Xie, X. Wang, and G. Yan, "An easy-to-use airborne lidar data filtering method based on cloth simulation," *Remote sensing*, vol. 8, no. 6, p. 501, 2016.